EPJ Web of Conferences **340**, 03007 (2025) https://doi.org/10.1051/epjconf/202534003007
Powders & Grains 2025

Magnetic shaking distributes granular particles homogeneously in microgravity

Fahad Puthalath[1,3,*], *Peidong* Yu[1,**], *Matthias* Schröter[2], and *Matthias* Sperl[1,3]

[1]Institut für Materialphysik im Weltraum, Deutsches Zentrum für Luft- und Raumfahrt (DLR), 51170 Köln, Germany
[2]Max Planck Institute for Dynamics and Self-Organization, Am Faßberg 17, D-37077, Göttingen, Germany
[3]Institut für Theoretische Physik, Universität zu Köln, 50937 Cologne, Germany

Abstract. This study investigates the dynamics of granular particles agitated by magnetic shaking within a drop tower setup. We analyze the experimental images showing approximately 450 spherical magnetic particles with a diameter of 1.6 mm in a 60 mm spherical sample cell. We find that the magnetic excitation leads to a uniform spatial distribution of both particle positions and velocities. This demonstrates the effectiveness of magnetic shaking as a method for controlling granular systems in microgravity environments, with potential applications in material science and space technology.

1 Introduction

One of the fundamental assumptions of the kinetic theory of granular gases is that particles exhibit a homogeneous spatial distribution, both in terms of their positions and velocities. To experimentally realize this condition, two key requirements must be met: gravity must be eliminated, and an excitation mechanism must be employed to uniformly distribute the particles in space. The former can be achieved using microgravity platforms, such as drop towers, parabolic flights, and sounding rockets [1–3]. For the excitation, shaking of the sample cell or cell boundaries has been used in most of the granular gas experiments in micro-gravity [1, 2]. However it has been shown that such shaking mechanisms may bring extreme inhomogeneity, as particles tend to cluster at the centre following collisions whereas near the boundaries particles have higher kinetic energy due to direct heating from shaken walls [1, 4]. In contrast, we used particles made from ferromagnetic material and used electromagnets to shake them once zero gravity is achieved. Through DEM simulations, we previously demonstrated how the strength of the magnetic field, the shape of the sample cell, and the influence of interparticle dipole interactions contribute to achieving homogeneity [5, 6]. Following the conclusions from DEM simulations, experiments were repeated in a Drop-tower campaign in Bremen, operated by the Center of Applied Space Technology and Micro-gravity (ZARM) [7] of the University of Bremen. In this paper, we examine an experiment from the campaign where metallic particles are levitated in a spherical sample cell. These particles are driven into motion by eight surrounding magnets and subsequently cool down due to energy dissipation from collisions with one another and the sample cell boundary after the magnets are turned off. We utilize a Convolutional Neural Network (CNN) with a U-Net architecture, trained with our experimental data, to detect the positions of particles in the images. The detected particle positions are then used in our analysis to demonstrate the spatial homogeneity achieved in the experiment.

2 Experiment setup

The experiment utilizes a spherical sample cell made of polymethyl methacrylate (PMMA) with a diameter of 60 mm, containing nearly 450 spherical Mu-Metal particles, each with a diameter of 1.6 mm. The sample cell is mounted between 8 electromagnets placed at the corners of a cube, as illustrated in Fig. 1, which depicts the experimental setup. To achieve homogeneous mixing of the particles during the Drop Tower experiment, a magnetic shaking protocol is employed. The shaking protocol consists of a 20 ms pulse of DC voltage applied to a single pair of diametrically opposite magnets, followed by an 80 ms relaxation period. This sequence is repeated for each of the four pairs of magnets, with a total cycle time of 400 ms. The low coercivity of the Mu-Metal particles ensures that long-range interactions between particles are negligible during the cooling phase, while during the heating phase, these interactions contribute to a more isotropic distribution of particles, as demonstrated in our previous work[5, 6]. The ZARM Drop tower provides a reduced gravity condition of $10^{-6}g$ ($g = 9.8m/s^2$) for approximately 9.4 seconds. The shaking protocol is applied during the first half of the microgravity phase, and the particles are allowed to evolve freely during the second half. The particle dynamics is captured with a CMOS camera EoSens 4CXP from Mikrotron GmbH at a framerate of 165 fps.

*e-mail: fahad.puthalath@dlr.de
**e-mail: peidong.yu@dlr.de

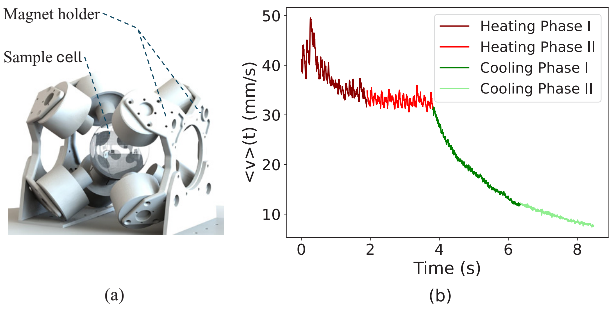

Figure 1: (a) Sample cell setup with 8 magnets, The magnets are arranged in a cubic configuration to provide a uniform magnetic field, and agitation is performed contactless from the outside without moving parts. (b) Temporal variation of average velocity, categorized into four phases. Cooling starts in the second half of the experiment, when the average velocity has stabilized at a constant value, with negligible fluctuations.

3 Data analysis

Images are recorded during the whole run of the the experiment: from the initial heating phase (Fig.2a) to the final cooling phase (Fig.2b). Upon examining the images, we encounter a significant challenge in analyzing them. The magnet arrangements in our setup limit our ability to achieve optimal lighting conditions. Additionally, the metallic particles used in the experiment can reflect light, making it challenging to accurately segment the images. Close inspection of the images shows that the reflection of light from the particle surfaces makes it difficult to distinguish between the particles and the background. Initial attempts with usual image processing methods, such as binarization, erosion and dilation, proved insufficient for accurately segmenting the particles from the background. However, by leveraging the capabilities of deep learning, we were able to significantly improve our results. Inspired by a recent study that successfully applied U-Net to particle identification in granular experiments[8], we adopted a U-Net model implemented using Tensorflow [9] libraries for our image segmentation task. The U-Net architecture, is a convolutional neural network (CNN) initially developed for medical image segmentation [10].

We train the U-Net model from scratch using a dataset of 20 experimental images, selected at different points in time, and their corresponding binary ground truth images, which classify pixels as either particles or background. To facilitate efficient processing and reduce memory requirements, each image is divided into smaller tile images, resulting in approximately 10,000 training images with a dimension of 128×128 pixels. Our model is trained using the Adam optimizer, with a sigmoid activation function at the output layer, and we use Binary Cross-Entropy as loss function.

An optimal model is chosen by fine-tuning hyperparameters to get the best value for recall and precision, and is used to make predictions on raw images. Subsequently, the output images from the network are further processed to get particle coordinates in each frame (Fig.2c). Once we have the particle coordinates in each frame, we need to match the particle positions across frames to track their movement. While U-Net facilitates the extraction of particle coordinates, particle tracking through the frames remains a challenging task due to the frequent overlap of particles in the images. However, here we employ a simplified approach to estimate particle velocities in individual frames. We calculate the instantaneous velocity (2D projection) of particles by comparing subsequent frames and assigning each particle's next position as their nearest neighbor in the subsequent frame. This is done by creating a list of possible mappings between frames, selecting closest pairs within a threshold distance, and removing duplicate assignments. However, using a low threshold cutoff underestimates particle movements, as it may not capture the true motion of the particles. In contrast, a threshold cutoff of approximately 0.5 times the particle diameter allows us to map local velocities for over 97% of particles, and increasing this value does not improve the results. Fig. 1b shows average velocity data calculated through this method over the whole duration of the experiment.

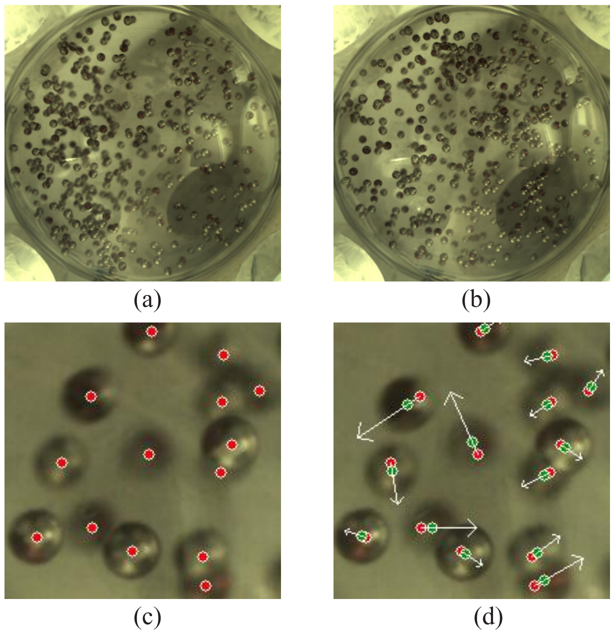

Figure 2: The progression from the initial magnetic heating phase (a) to the cooling phase (b) reveals a more uniform distribution of particles over time. The application of U-Net for particle detection yields accurate particle positions (red dots) (c). Furthermore, tracking the particles into the next frame (green dots) and analyzing the corresponding displacement vectors (d)(scaled up 5 times for visibility), reveals a random, isotropic distribution of velocity directions.

4 Results

Previous DEM simulation results from our group have demonstrated the effectiveness of the 8-magnet setup as a thermostat in achieving homogeneous particle distribution [5, 6]. These findings are corroborated by the experimental results presented here. We present the results of our image analysis, including the spatial distribution of particle positions and the mean velocity profiles in different regions of the sample cell.

4.1 Distribution of particle positions

The particle number density distribution exhibits distinct differences between the cooling and heating phases. During the heating phase, as illustrated in Fig.3a, a distinct 4-fold symmetric pattern, characterized by increased particle densities near the sample cell corners appears. This pattern is consistent with the expected response of particles to the applied magnetic forces. These high-density regions disappear during cooling, as shown in Fig.3b. The remaining subtle inhomogeneities can be identified as inelastic clustering, which is expected during the cooling process. The slight decrease in density in the outermost layer is due to the presence of the cell boundary which creates an excluded volume. The data shown are normalized considering the varying depth of the sample cell at different positions, and is averaged over a time duration of 3 seconds, corresponding to 495 image frames.

This outcome differs from boundary-driven shaking, where clustering often occurs at the sample cell center [1]. Although short-range clustered regions are present during cooling, the short time frame of our study does not allow for the formation of large-scale clusters.

4.2 Distribution of particle velocities

The kinetic theory assumes that particles exhibit homogeneity in both their positions and velocities, meaning that velocities should be uniformly distributed across the space. Fig.4 shows the velocity magnitudes averaged over a 1-second duration for particles reaching each polar sector during heating and cooling. Data shown are taken from the phase II of heating and cooling (as shown in Fig. 1b), where minimal fluctuation is observed for the mean velocity magnitude. The mean velocity magnitude decays by approximately 2 mm/s during this time, which is less than the fluctuations observed during heating, justifying our selection of the time range for obtaining sufficient data for the distribution. From the figure, it can be easily observed that the velocities are indeed uniformly distributed in both the heating and cooling phases. Which means that the intermittent shaking mechanism we employed does not lead to an accumulation of particles with high velocities close to the magnets.

This result can be motivated by the actual driving protocol: the heating phase with a pair of magnets turned on extends only 20 ms, and although particles are pulled to the adjacent volume during this phase, their collisions within this region sufficiently mix the velocities during the subsequent 80 ms relaxation phase, resulting in a uniform velocity distribution.

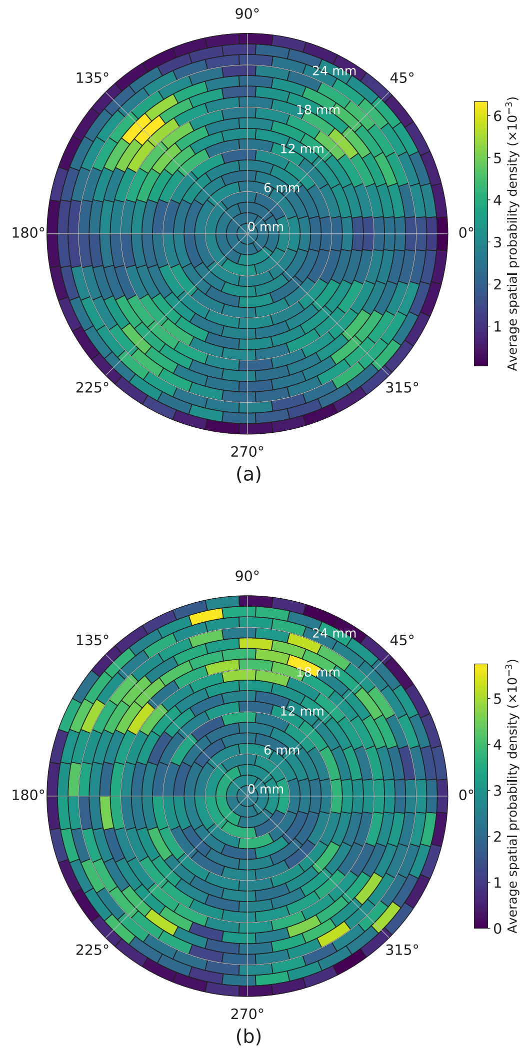

Figure 3: The number density, normalized by depth of the sphere, exhibits distinct differences between the two phases: (a) Averaged during the last 3 seconds of the heating phase, density fluctuations with fourfold symmetry emerge, whose positions reflect the symmetry of the driving magnet arrangement. (b) In contrast, averaged during the last 3 seconds of cooling, the fourfold symmetry observed in the heating phase disappears, and new, less pronounced inhomogeneities arise, likely due to inelastic clustering.

5 Conclusion

We have successfully demonstrated that intermittent shaking of magnetic granular particles using our 8-magnet setup promotes a homogeneous distribution, which is achieved through the interplay of magnet switching and random particle collisions during the turn-off phase, where the switching of magnets leads to long-term isotropy and

 https://doi.org/10.1051/epjconf/202534003007

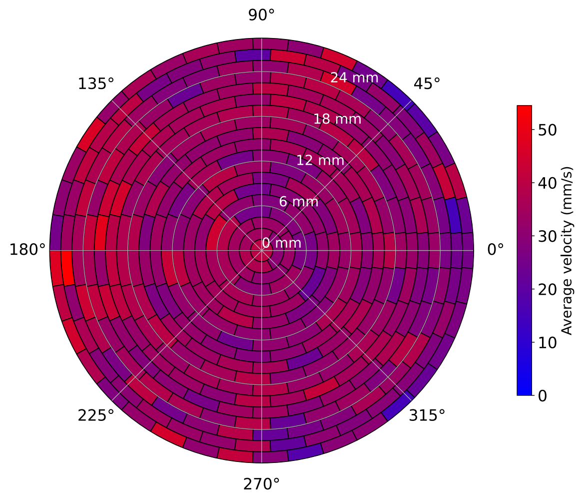

Figure 4: Magnitude of particle velocities averaged over 1 second duration, showing a uniform distribution across different regions of the sample cell, which is divided into equal area polar sectors. Unlike the position distribution, the velocity distribution lacks concentrated regions, indicating that the intermittent shaking mechanism effectively suppresses the formation of velocity gradients. The uniformity of the velocity distribution is evident in both the heating (a) and cooling (b) phases, suggesting that the system has achieved a high degree of spatial uniformity in its velocity field.

the collisions absorb excess kinetic energy and randomize motion. We believe that our ability to create a homogeneous mixture of granular particles opens up new opportunities for experimental studies of granular gas dynamics, particularly in the context of freely cooling systems. With a well-controlled and uniform initial state, it may be possible to observe the emergence of complex structures and patterns in granular gas, as observed in simulations.

References

[1] E. Falcon, R. Wunenburger, P. Évesque, S. Fauve, C. Chabot, Y. Garrabos, D. Beysens, Cluster formation in a granular medium fluidized by vibrations in low gravity, Phys. Rev. Lett. **83**, 440 (1999). 10.1103/PhysRevLett.83.440

[2] M. Hou, R. Liu, G. Zhai, Z. Sun, K. Lu, Y. Garrabos, P. Evesque, Velocity distribution of vibration-driven granular gas in knudsen regime in microgravity, Microgravity Science and Technology **20**, 73 (2008). 10.1007/s12217-008-9040-5

[3] P. Yu, M. Schröter, M. Sperl, Velocity distribution of a homogeneously cooling granular gas, Phys. Rev. Lett. **124**, 208007 (2020). 10.1103/PhysRevLett.124.208007

[4] A. Kudrolli, M. Wolpert, J.P. Gollub, Cluster formation due to collisions in granular material, Phys. Rev. Lett. **78**, 1383 (1997). 10.1103/PhysRevLett.78.1383

[5] M. Adachi, P. Yu, M. Sperl, Magnetic excitation of a granular gas as a bulk thermostat, npj Microgravity **5**, 19 (2019). 10.1038/s41526-019-0079-y

[6] M. Adachi, M. Balter, X. Cheng, J. Drescher, X. Li, M. Sperl, S. Zhao, P. Yu, Characteristics of a magnetic bulk thermostat for granular gas investigations in microgravity, Microgravity Science and Technology **33**, 11 (2021). 10.1007/s12217-020-09853-5

[7] M. Cornelius, ZARM drop tower Bremen User manual, ZARM Drop Tower Operation and Service Company (2023)

[8] N. Sanvitale, C. Gheller, E. Bowman, Deep learning assisted particle identification in photoelastic images of granular flows, Granular Matter **24**, 65 (2022). 10.1007/s10035-022-01222-w

[9] M. Abadi, A. Agarwal, P. Barham, E. Brevdo, Z. Chen, C. Citro, G.S. Corrado, A. Davis, J. Dean, M. Devin et al., TensorFlow: Large-scale machine learning on heterogeneous systems (2015), software available from tensorflow.org, `https://www.tensorflow.org/`

[10] O. Ronneberger, P. Fischer, T. Brox, U-net: Convolutional networks for biomedical image segmentation (2015), `1505.04597`, `https://arxiv.org/abs/1505.04597`